Journal of Materials Chemistry B

ROYAL SOCIETY OF CHEMISTRY

REVIEW

View Article Online
View Journal | View Issue



Cite this: J. Mater. Chem. B, 2022, 10, 7450

# Recent advances in nanotechnology mediated mitochondria-targeted imaging

Nannan Zheng,[a] Qinghui Wang,[a] Shijin Zhang,[a] Chenchen Mao,[b] Liangcan He *[a] and Shaoqin Liu *[a]

Received 29th April 2022,
Accepted 13th July 2022

DOI: 10.1039/d2tb00935h

rsc.li/materials-b

Mitochondria play a critical role in cell growth and metabolism. And mitochondrial dysfunction is closely related to various diseases, such as cancers, and neurodegenerative and cardiovascular diseases. Therefore, it is of vital importance to monitor mitochondrial dynamics and function. One of the most widely used methods is to use nanotechnology-mediated mitochondria targeting and imaging. It has gained increasing attention in the past few years because of the flexibility, versatility and effectiveness of nanotechnology. In the past few years, researchers have implemented various types of design and construction of the mitochondrial structure dependent nanoprobes following assorted nanotechnology pathways. This review presents an overview on the recent development of mitochondrial structure dependent target imaging probes and classifies it into two main sections: mitochondrial membrane targeting and mitochondrial microenvironment targeting. Also, the significant impact of previous research as well as the application and perspectives will be demonstrated.



## 1. Introduction

Known to be the cell's main energy supply organelles, mitochondria are the primary source of intracellular reactive oxygen species and are responsible for modulation of apoptosis.[1,2] Also, mitochondria are closely associated with many diseases involving cellular energy disorders and oxidative damage, such as neurodegeneration, cardiovascular diseases and metabolic

[a] School of Medicine and Health, Key Laboratory of Microsystems and Microstructures Manufacturing (Ministry of Education), Harbin Institute of Technology, Harbin, 150001, China. E-mail: liangcanhe@hit.edu.cn, shaoqinliu@hit.edu.cn
[b] Department of Electrical, Computer and Energy Engineering, University of Colorado Boulder, Boulder, Colorado, 80303, USA

**Nannan Zheng**

*Dr Nannan Zheng obtained her PhD in Biomedical Engineering from Harbin Institute of Technology in 2021. After graduation, she started her postdoctoral career at Harbin Institute of Technology. Her research interests are mainly focused on the multifunctional nanoparticles for cancer diagnosis and therapy. Dr Zheng's research also focuses on nanoparticles for the treatment of Alzheimer's disease.*

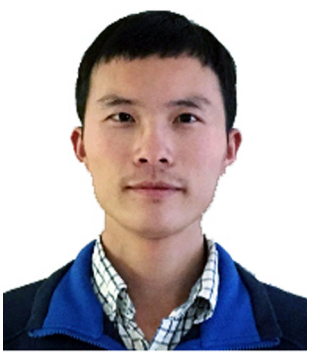

**Liangcan He**

*Dr Liangcan He graduated from Tsinghua University and National Center for Nanoscience and Technology in 2014 under the guidance of Prof. Zhiyong Tang and Prof. Yadong Li. After that, he joined Prof. Jennifer N. Cha's group in the University of Colorado, Boulder, as a Research Associate, and later worked with Prof. Jennifer N. Cha and Prof. Christopher N. Bowman as a Senior Research Associate. In June 2018, he joined Dr Shawn Chen's lab in the National Institutes of Health as a Postdoc Research Scientist. In May 2021, he started his independent career at Harbin Institute of Technology. His research interests focus on design and synthesis of organic–inorganic nanomaterials for biomedical applications.*

diseases.[3–5] To gain a deeper understanding of the diagnosis and treatment of these diseases, mitochondrial movement and dynamic changes have drawn intense research with recent advances in mitochondrial research, bioenergetics and metabolism, reactive oxygen species and cell signal detection. However, since the ultrastructure of mitochondria is typically close to the diffraction limit in optical microscopy, it would be challenging to directly observe submitochondrial architecture or protein distributions using standard light microscopes. As a result, there is a substantial lack of research and study on subcellular organelles. Thanks to the development of mitochondria-targeted imaging techniques and more advanced microscopy technology, changes in the internal microstructure of mitochondria are gradually becoming better understood. Currently, the techniques used in mitochondria-targeted imagingt mainly include implementing small molecule fluorescent probes, polypeptide fluorescent probes, and nanoscale fluorescent probes. The fluorescent probes can be modified to exhibit multifunctional properties, such as anti-tumor therapy function, and selective targeting mitochondrial reactive oxygen species and reductive species attachment.[6–8] To be specific, small molecule fluorescent probes, such as commercial MitoTrack ®Green FM and Rhodamine 123, JC-1, are mainly modified by cations to enable them to locate and image mitochondria. Additionally, mitochondria targeted imaging can also be achieved by the introduction of mitochondrial targeting groups, such as triphenyl-phosphine (TPP)-Green,[9] IR-780 iodide,[10] CAI,[11] *etc.* As regards polypeptide fluorescent probes, the mitochondrial localization and fluorescence imaging functions can readily be realized by linking the polypeptides with the fluorophore groups.[12] Although various organic fluorescent probes have been used for mitochondrial imaging, the development of fluorescent probes with low toxicity, high selectivity and excellent photostability still face challenges. In recent years, with the rapid development of nanotechnology, nanomaterial-based probes not only offer the advantages of commercial mitochondrial imaging, but also can be designed to respond to the changes in the mitochondrial microenvironment. Mitochondrial imaging based on nanotechnology mainly includes targeting mitochondrial structures (such as the mitochondrial outer membrane, mitochondrial inner membrane, cristae, and mtDNA) and targeting the mitochondrial microenvironment (ATP, pH, and ROS) and signaling molecules ($H_2S$). Mitochondria-targeted imaging is useful in a wide range of applications, including long-term imaging of living mitochondria, exploration of the changes in the mitochondrial structure, microenvironment investigation and treatment for diseases. Here, this paper will review the recent progress on the application of nanomaterials in mitochondrial imaging and elaborate the advantages of nanomaterial implemented mitochondrial imaging by exploring the structural and microenvironmental alterations in mitochondria. This review aims to understand and propose new directions of nanomaterial engineering for the study of mitochondria-related diseases. It is organized in three parts: the first one reviews and discusses the mitochondrial targeting imaging of mitochondrial membrane; the second part is dedicated to microenvironmental imaging. Last, our conclusions and proposals for new generation of technology will be presented in the final section.

## 2. Mitochondrial membrane targeting imaging

The structure of mitochondria can be divided into four functional regions: mitochondrial outer membrane (OMM), mitochondrial inner membrane (IMM), mitochondrial intermembrane space (IMS), and mitochondrial matrix (MM).[3,13,14] The design of various small-molecule mitochondrial targeting probes is realized by exploiting the negative potential of the mitochondrial membrane. Consequently, the fluorescent probes that target the mitochondrial outer membrane mainly include actin chromobody targeting,[15] mitochondrial membrane potential[16–18] and monoamine oxidase.[19,20]

Due to the oxidation pathway and proton pump operation, mitochondria have a very large membrane potential, reaching up to −180 mV, which is 5–6 times that of the plasma membrane and is quite different from those of other biological membranes.[21] Therefore, cationic compounds are more easily labeled in mitochondria than in other organelles,[22] which is the reason why cationic fluorescent compounds such as triphenylphosphorous ($TPP^+$), tetramethylrhodamine methyl ester (TMRM), tetramethylrhodamine ethyl ester (TMRE) and 5,5′,6,6′-tetrachloro-1,1′,3,3′-tetraethylbenzimidazolcarbocyanine iodide (JC-1),[23,24] (*E*)-4-(1*H*-indol-3-ylvinyl)-*N*-methylpyridiniumiodide (F16),[25,26] dequalinium (DQA),[27,28] Rhodamine[29,30] and guanidine/biguanidine[31] have excellent mitochondrial targeting performance. Therefore, grafting mitochondrial targeting molecules such as triphenylphosphine onto the surface of nanoparticles is a simple strategy to obtain mitochondrial targeting nanoprobes.

Lanthanide doped upconversion nanoparticles (UCNPs) can emit high energy UV or visible light under excitation of near-infrared light, which has the potential for biomedical imaging applications.[32,33] However, undecorated UCNPs cannot localize to mitochondria to achieve the function of disease diagnosis and treatment. Recently, Zhao's group synthesized Janus nanostructures by growing porphyrin MOF on $Nd^{3+}$ sensitized upconversion nanoparticles (UCMTs) and the mitochondrial targeting function was achieved by surface modification of triphenylphosphine[34] (Fig. 1). In this work, mitochondria-targeted PDT induces the initiation of endogenous apoptotic pathways, resulting in a superior therapeutic effect to that of untargeted therapies.

Black phosphorus (BP) is a novel bioinorganic material with biocompatibility, biodegradability and biosafety. It has been used as a photothermal agent for cancer treatment due to its extensive near infrared absorption.[35–37] There is still plenty of potential to improve the therapeutic efficacy of nanomedicine based on BP. In 2018, Dong's group developed an image-guided mitochondrial targeted photothermal/photodynamic nanosystem[38] (Fig. 1). Based on dopamine-coated black phosphorus nanosheets,

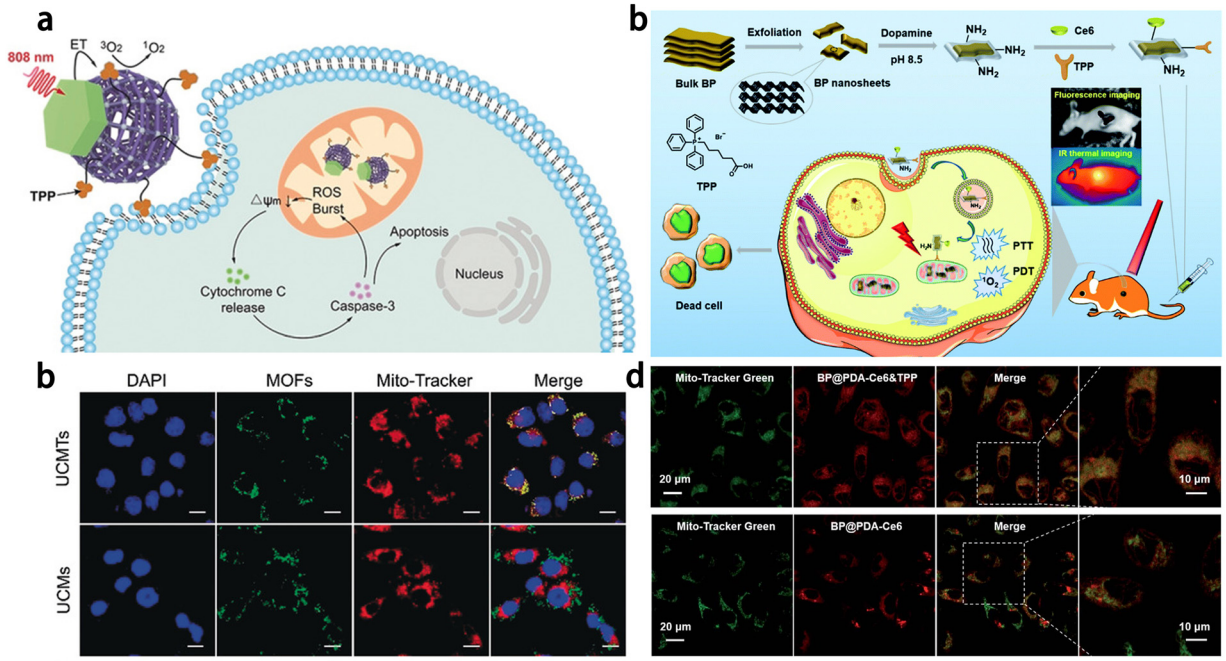


Fig. 1 (a) Schematic of mitochondria-targeted upconversion MOFs for amplified PDT. (b) Confocal fluorescence images of the 4T1 cells treated with UCMTs or UCMs. The green fluorescence is from the MOFs.[34] (c) Schematic illustration of the preparation and therapeutic functions of BP@PDA-Ce6&TPP NSs. (d) Confocal fluorescence images of HeLa cells incubated with BP@PDA-Ce6&TPP NSs and BP@PDA-Ce6 NSs (excited at 633 nm) and then Mito-Tracker Green (excited at 488 nm).[38] Copyright 2019, wiley and 2018, Royal Society of Chemistry.

the system covalently linked with Ce6 and TPP to form BP@PDA-Ce6&TPP NSs. TPP modification significantly improved the mitochondrial targeting ability of BP@PDA-Ce6&TPP NSs, and its killing efficiency against tumor cells was significantly improved.

In addition, Zhuang *et al.* prepared a mitochondrial targeting fluorescent probe AuNC@CS-TPP by combining chitosan-modified Au nanocrystals (AuNC@CS) with TPP through covalent bonding.[39] The conjugated compound AuNCs@CS-TPP emits blue fluorescence at 440 nm with a high quantum yield of 8.5%. It is noteworthy that the fluorescence intensity of AuNCs@CS-TPP labeled HeLa cells showed insignificant quenching after irradiation for 8 min, demonstrating its high photostability.

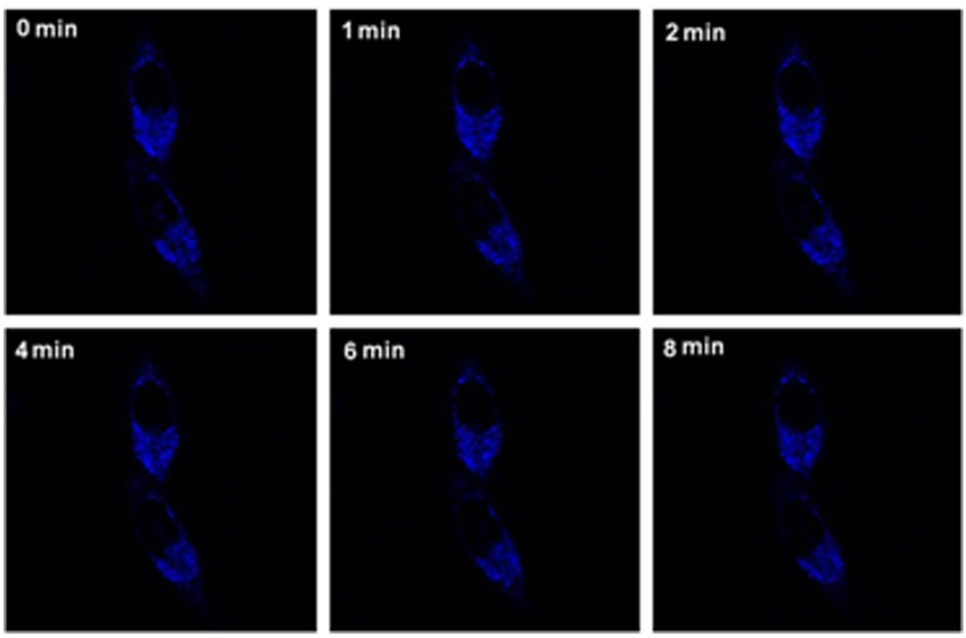


Fig. 2 Fluorescent images of living HeLa cells cultured with AuNCs@CS-TPP (20 μg $mL^{-1}$) with various incubating times (0–8 min). Excitation wavelength: 405 nm. Reproduced with permission.[39] Copyright 2014, Elsevier.

 

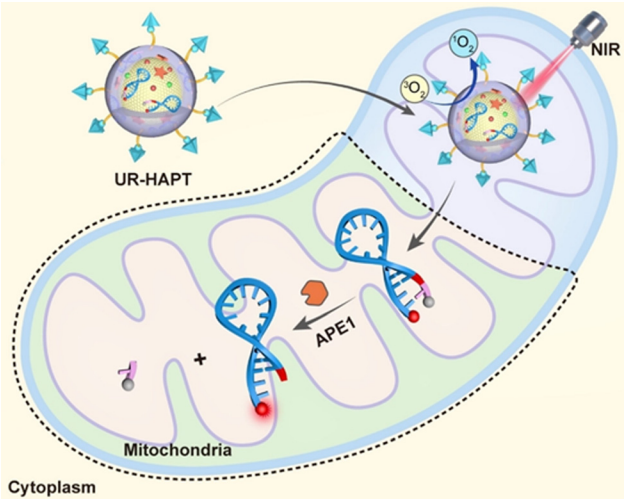


Fig. 3 Schematic illustration of the design of UR-HAPT for precise imaging of subcellular enzymatic dynamics of APE1 during NIR light-mediated, mitochondria-targeted PDT.[40] Copyright 2022, Wiley-VCH GmbH.

Moreover, the studied compound AuNC@CS-TPP can accumulate selectively in the mitochondria of HeLa and HepG2 cells, which suggests its potential for targeted imaging of mitochondria in live cells (Fig. 2). The laser confocal microscope is used in Fig. 2. Combining TPP with traditional nanomaterials, mitochondrial targeting function can be endowed with nanomaterials to achieve mitochondrial imaging and therapeutic effects.

Yu *et al.* constructed a multifunctional nanoplatform (called UR-HAPT) by combining ucNP-based nano-photosensitizer and mitochondrial targeting strategy with a reasonably designed DNA reporter (Fig. 3).[40] The platform enables simultaneous monitoring of the subcellular dynamics of human apurinic/apyrimidinic-free endonuclease 1 (APE1) during near-infrared (NIR) light-mediated PDT. APE1 accumulation in mitochondria can be visualized during PDT *in vitro* and *in vivo*. Thus, it can be used to screen and evaluate potential enzyme inhibitors to improve the efficacy of PDT.

There have been a wide variety of TPP-based compounds that have proved to be useful for mitochondria-targeted imaging, such as NIR Cy-5-TPP/FF,[41] WSSe/$MnO_2$-INH-TPP@CM,[42] C-dots-TPP[43] and Gold-TPP.[44]

In addition to TPP, which can be used as a small molecular group targeting the mitochondrial outer membrane, PQC is also a group that can target mitochondria. Tang *et al.*[45] designed lipid small molecule hybrid nanoparticles (LPHNPs) for imaging and treatment of *in situ* glioma models. LPHNPs are prepared by designing a co-assembly of lipids and amphiphilic pheophorbide a-quinolinium conjugate (PQC), a small-molecule-specific mitochondria (Fig. 4). Unlike PQC-NFS, LPHNPs exhibit a spherical nanostructure and ideal particle size, which reduces potential systemic toxicity and enables the administration of nanoparticles by intravenous injection. In addition, compared to traditional liposomes, LPHNPs have a higher drug loading and better stability, and retain the excellent properties of PQC, such as mitochondrial targeting, fluorescence imaging ability and photosensitivity. By integrating the benefits of liposomes and PQC molecules, LPHNPs achieve minimal systemic toxicity, enhanced photodynamic therapy (PDT) efficacy, and the ability to visualize drug biologic distribution and tumor imaging. Mixed nanoparticles showed good efficacy and could significantly prolong the survival time of mice with glioma *in situ*. Fluorescence imaging showed that LPHNPs accumulated at the tumor site 2 hours after injection and remained there for at least 48 hours. *In vitro* imaging further confirmed the tumor-targeting ability of LPHNPs. In an *in situ* glioma model, single-dose LPHNPs combined with laser therapy have a good inhibitory effect on tumor progression. More importantly, they

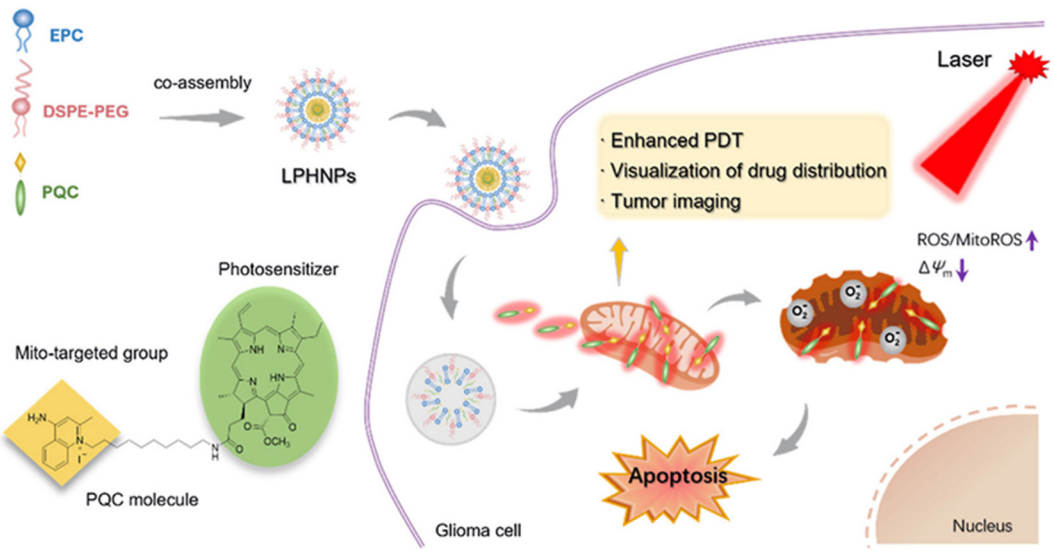


Fig. 4 Schematic illustration of hybrid nanoparticles (LPHNPs) based on amphiphilic lipids and mitochondria targeting PQC molecules.[45] Copyright 2022, Elsevier.

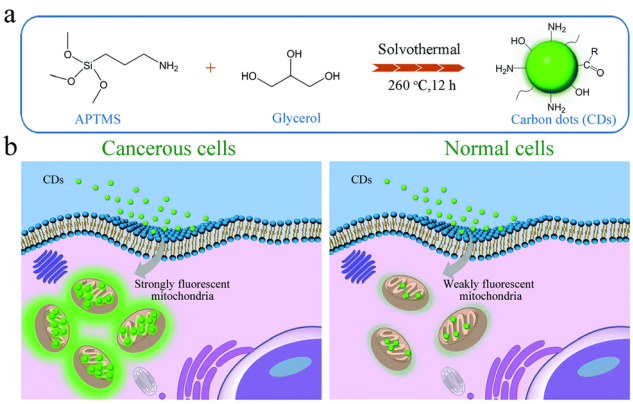


Fig. 5 One-step solvothermal synthesis of APTMS CDs using APTMS and glycerol and applications of APTMS CDs in mitochondrial tracking and normal/cancerous cell differentiation.[46] Copyright 2017, Royal Society of Chemistry.

significantly extended the survival time of mice with glioma *in situ*. The unique co-assembly of lipids and small molecules offers a new potential for the construction of new liposome derived nanoagents and improved cancer therapy.

In addition, the construction of a positively charged surface environment for nanomaterials is another strategy for designing mitochondrial membrane targeted imaging nanoprobes. In 2017, Wu's group prepared fluorescent carbon quantum dots (APTMS CDs) with the mitochondrial targeted imaging function by solvent heat treatment of glycerol and organosilane molecules (3-aminopropyl)trimethoxysilane (APTMS).[46] The abundant amino groups on the surface of APTMS CDs lead to a zeta potential of +13.1 mV in water, endowing them with the ability for mitochondrial targeting. Compared with normal cells, cancerous cells have a more negative mitochondrial membrane potential of about −220 mV,[47,48] resulting in a stronger electrostatic interaction between APTMS CDs and mitochondrial membrane, and so a brighter fluorescence can be observed in cancerous cells (Fig. 5). Therefore, APTMS CDs can be used to distinguish normal cells and cancerous cells.

# 3. Mitochondrial microenvironment imaging

## 3.1 Mitochondrial matrix targeted imaging

Mitochondria matrix is the main structure of mitochondria, and contains numerous proteins/enzymes, nucleic acids, hydrogen sulfide and other biological species for energy supply and signal transduction. These components serve as a medium for mitochondrial imaging.[49,50] In order to prolong the retention time of the fluorescence in mitochondria, Grzybowski and Kandere-Grzybowska *et al.* designed mixed-charged nanocarriers for selective targeting of mitochondria by otherwise nonselective dyes.[51] In this work, the mixed-charged nanocarriers traverse an endolysosomal tract to selectively deliver non-covalently bound dye molecules into mitochondria and covalently link them to cysteines of mitochondrial proteins *via* disulfide bonds (Fig. 6).

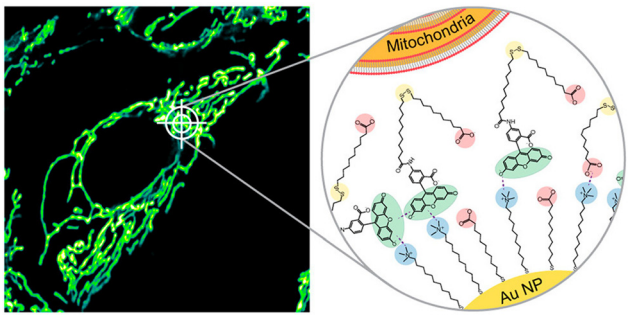


Fig. 6 Mechanism of action of mixed-charge nanocarriers targeting mitochondria.[51] Copyright 2021, American Chemical Society.

It is also demonstrated that the nanoparticles of interest can deliver low-toxicity anionic fluorophores into mitochondria to observe the dynamic remodeling process of mitochondrial network and even long-term tracking of mitochondria in dividing cells. Cell mitochondria are imaged using confocal laser scanning microscopy (CLSM).

## 3.2 ATP targeting imaging

Adenosine triphosphate (ATP) consists of three main components: adenine, ribose, and three phosphate groups. When hydrolyzed, a large amount of energy is released, providing a direct source of energy for metabolism and activity.[52,53] Mitochondria are the major organelles that produce ATP;[54] therefore, mitochondrial imaging can be achieved by monitoring the fluctuation of ATP level in mitochondria or the fluctuation of cellular ATP levels. Chu and coworkers developed a fluorescent ATP probe out of titanium carbide (TC) nanosheets that had been modified with an ROX (X-rhodamine)-labeled ATP aptamer (TC/Apt).[55] TC in the TC/Apt shows superior quenching efficiency for ROX (*e.g.*, ∼97%). In the presence of ATP, the ROX-tagged aptamer is released from the TC surface, resulting in the recovery of ROX fluorescence under 545 nm excitation (Fig. 7). Through this procedure, the researchers successfully obtained the fluorescence detection and imaging of ATP in living cells, body fluids (*e.g.*, urine and serum), and a mouse tumor model.

Deng *et al.* reported the imaging of subcellular mitochondria and mitochondrial ATP in living cells[56] targeted by nano-ZIF-90 that self-assembled from $Zn^{2+}$ and imidazole-2-carboxyaldehyde (2-ICA). After ATP triggering the breakdown of ZIF-90, the encapsulation of fluorescent Rhodamine B (RhB) into ZIF-90 inhibits the emission of RhB. The release of RhB for ATP induction is caused by a competitive coordination between ATP and the metal nodes of ZIF-90 (Fig. 8). The electrostatic interaction between the positively charged ZIF-90 and the negatively charged mitochondria inner membrane facilitates the accumulation of RhB/ZIF-90 within mitochondria. This method allows for imaging mitochondrial ATP in living cells and studying fluctuations in ATP levels during glycolysis and apoptosis.

In addition, graphene quantum dots (GQDs), as a new class of carbon-based quantum dots, have unique properties such as stable photoluminescence, low toxicity and good biocompatibility.

 

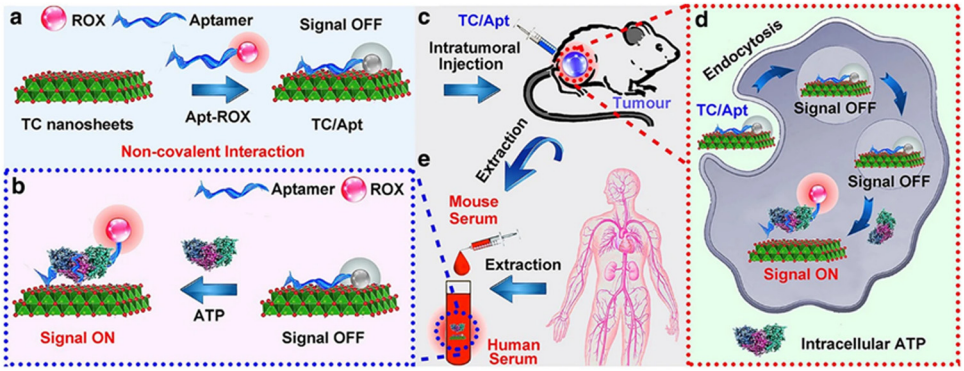


Fig. 7 Scheme of TC/Apt fluorescent probes. (a) Schematic diagram of fabrication of TC/Apt-based fluorescent probes. (b) TC/Apt-based fluorescent probes for the accurate detection of ATP based on a signal off/on switch mechanism. (c) TC/Apt-based fluorescent probes for *in vivo* imaging of ATP in tumors of a mouse model. (d) TC/Apt-based fluorescent probes for imaging analysis of intracellular ATP in live cells. (e) TC/Apt-based fluorescent probes for quantitative detection of ATP in real samples, such as mouse and human serum. Reproduced with permission.[55] Copyright 2021, Biomedcentral.



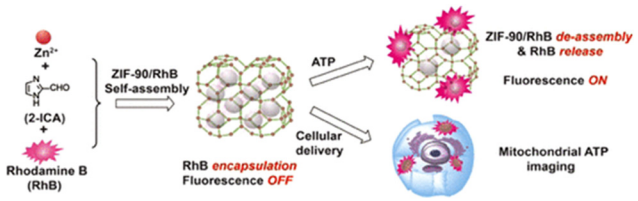


Fig. 8 Schematic representation of modulating the host–guest chemistry of nanoscale RhB/ZIF-90 for fluorescent ATP sensing and mitochondrial ATP imaging. Reproduced with permission.[56] Copyright 2017, American Chemical Society.

It can effectively avoid the limitation of poor luminescence stability of organic probes and has a great potential for mitochondrial targeted imaging. Liu *et al.* synthesized single-layered graphene quantum dots (s-GQDs) with yellow fluorescence for ATP imaging in living cells.[57] Macrocyclic aromatic conjugated structure and positively charged sites in s-GQDS can achieve specific recognition of ATP/GTP and good mitochondrial targeting ability. The results showed that s-GQDS successfully monitored the ATP fluctuation in HeLa cells after $Ca^{2+}$ and sodium azide treatment, respectively. This study offers an effective solution to monitor mitochondrial ATP fluctuations caused by ATP activation and inhibition in active cells. In other words, s-GQDs provide a new platform for studying cell metabolism diseases and mitochondrial dysfunction conditions.

### 3.3 $H_2O_2$ targeting imaging

As an important member of intracellular active species, hydrogen peroxide is one of the key by-products of energy metabolism. The physiological levels of hydrogen peroxide act as a molecular messenger and provide essential information for the regulation of intracellular processes, such as immune cell activation and vascular remodeling in mammals. There has been a link established between high levels of hydrogen peroxide and major diseases such as malignant tumors, neurodegenerative Parkinson's disease and Alzheimer's syndrome. Therefore, it is of great significance to detect the concentration levels of hydrogen peroxide in mitochondria for the prevention, diagnosis and pathological studies of certain diseases. The ratiometric fluorescence technique based on the fluorescence resonance energy transfer (FRET) mechanism is highly accurate and shows significantly low interference, thus enabling real-time detection and imaging of hydrogen peroxide in mitochondria. Wu and coworkers designed a multifunctional fluorescent nanoprobe for detecting mitochondrial $H_2O_2$.[58] A mitochondria-targeting ligand (TPP) and an $H_2O_2$ recognition element (PFl) are covalently linked onto carbon dots to construct the nanoprobe (CDs). Mito-CD-PF1 is non-cytotoxic and easily loaded into cells for ratiometric detection of mitochondrial $H_2O_2$ variations in the presence of exogenous or endogenous $H_2O_2$ (Fig. 9). This work offers some important insights into the design and construction of fluorescence detection and imaging system at the subcellular level. Another example of FRET based imaging was presented by Niu and Qiao.[59] In their work, the ratiometric detection of mitochondrial $H_2O_2$ in live cells was successfully realized by the introduction of a self-assembled polymeric micelle that carried tetraphenylethene (TPE), fluorescent boronate and triphenylphosphonium as the donor, a $H_2O_2$-responsive acceptor, and a mitochondria-targeted moiety, respectively. To further extend the study, one can incorporate multi-functional molecules into the nanoprobes to enable them to be accessible for targeting, sensing, and energy transfer.

### 3.4 $H_2S$ targeting imaging

Hydrogen sulfide ($H_2S$) is a multipurpose regulator in cells and is involved in a variety of diseases caused by mitochondrial dysfunction.[60,61] As the major metabolic locus of $H_2S$ in organisms,[62] the concentration change of $H_2S$ indirectly reflects the function of mitochondria. Additionally, the active chemical properties of $H_2S$ can also be used as a medium for mitochondrial imaging and reflect the physiological and pathological states of mitochondria. Therefore, various imaging probes have been developed in order to evaluate the function of mitochondria through monitoring the level of $H_2S$ in mitochondria.[63–65] Currently, the organic molecule probes used

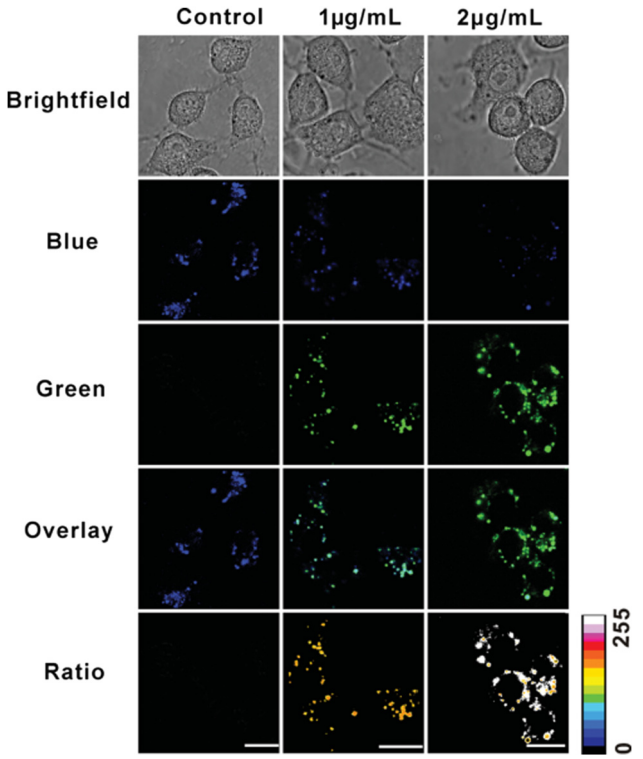


Fig. 9 Confocal fluorescence images of Mito-CD-PF1-stained Raw 264.7 cells upon stimulation by PMA with varied concentrations. Columns from left to right: control (cells with no PMA), cells treated with 1 μg $mL^{-1}$ and 2 μg $mL^{-1}$ PMA. Rows from top to bottom: brightfield channel, blue channel, green channel, overlay of blue and green channel, and ratio image, respectively. Concentration of Mito-CD-PF1 in culture media: 0.15 mg $mL^{-1}$. Images were acquired under 405 nm excitation and fluorescent emission windows: blue = 425–475 nm, green = 500–550 nm. Scale bar: 15 μm. Reproduced with permission.[58] Copyright 2013, Wiley-VCH GmbH.

for mitochondrial $H_2S$ imaging are not suitable for long-term imaging *in vivo* for multiple reasons. First, the organic molecule probes cannot be effectively penetrated by excitation irradiation. Second, they exhibit short blood circulation time. Last, they easily bind with proteins before even reaching target cells. To address these problems, there have been a growing number of reports that apply upconversion nanoparticles (UCNPs) in the field of bioimaging, owing to their unique properties of negligible photobleaching, deep penetration depth, and high resistance to autofluorescence interference.[66] In 2018, Huang *et al.* developed a lysosome-assisted mitochondrial targeting probe based on triphenylamine-merocyanine (TPAMC) modified UCNPs (TPAMC-UCNPs@PHIS-PEG) with an acid-activated targeting strategy for ratiometric detection and imaging of $H_2S$ in mitochondria.[67] In the imaging system, the absorption spectra of TPAMC matched well with the green upconversion luminescence (UCL), resulting in a strong luminescence resonance energy transfer (LRET) from UCNPs to TPAMC. Thus, only a weak UCL signal in the green channel was observed for TPAMC-UCNPs@PHIS-PEG nanoparticles under 980 nm excitation. In mitochondria, TPAMC on the surface of nanoparticles reacts with $H_2S$, and its adsorption decreases sharply, leading to the recovery of green UCL. In order to improve the stability of the nanoprobe in blood circulation, a poly(ethylene glycol) (PEG) shell composed of 1,2-distearoyl-*sn*-glycero-3-phosphoethanolamine-*N*-[methoxy-(poly(ethylene glycol))-2000] (mDSPE-PEG) and poly(L-histidine)-*b*-PEG (PHIS-PEG) were further coated on the surface of TPAMC-UCNPs. PEG shells reduce the possibility that TPAMC-UCNPs will adhere to biomolecules and endow it with acid-activated properties (Fig. 10). *In vitro* and *in vivo* experiments indicated that TPAMC-UCNPs@PHIS-PEG nanoprobe was able to be used not only for ratiometric UCL imaging of mitochondrial $H_2S$ generation in living cells, but also for monitoring mitochondrial $H_2S$ levels in colon cancer mouse models.

### 3.5 Other mitochondrial microenvironment targeting imaging

In the above sections, we have reviewed the development of study in mitochondrial microenvironments by targeting matrix, ATP, $H_2O_2$, and $H_2S$. In this section, we will focus on nanoprobes that target other microenvironmental factors, such as pH and peroxynitrite. Xu and Zhou prepared a nanoprobe by covalently linking a mitochondria-targeted ligand (triphenylphosphonium, TPP) and a pH recognition fluorescence indicator (rhodamine, RhB) onto the surface of $MoS_2$ quantum dots (QDs). $MoS_2$ QDs serve as a fluorescent reference for the ratiometric signal as well as a nanocarrier for the targeted ligand and pH fluorescent indicator in this multifunctional fluorescent nanoprobe. The pH-sensitive fluorescence of the RhB-based group was compared to the pH-resistant fluorescence of $MoS_2$ QDs for ratiometric pH detection. After absorption in live cells, the nanoprobe was able to label mitochondria with great precision, allowing for imaging and pH monitoring.[68] Peroxynitrite ($ONOO^-$) is a group of biological oxidants that play a role in both physiological and

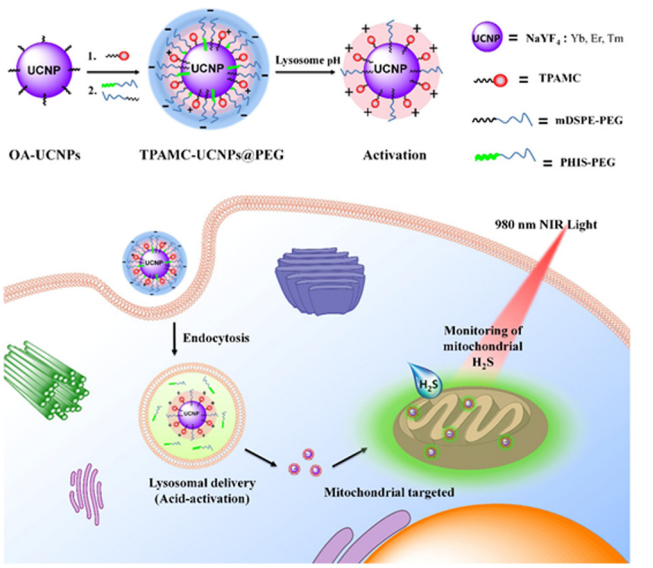


Fig. 10 Design of TPAMC-UCNPs@PEG, and the illustration of lysosome-assisted mitochondrial targeting process and UCL monitoring of mitochondrial $H_2S$ in cells. Reproduced with permission.[67] Copyright 2018, American Chemical Society.

 

pathological processes. It has proved difficult to detect $ONOO^-$ in biological systems due to its exceptionally short half-life and low steady-state concentration. Zhao and Yang prepared a ratiometric fluorescent nanoprobe for $ONOO^-$ by covalently connecting graphene quantum dots (GQDs) with cyanine 5.5 (Cy5.5). This nanoprobe (GQD-Cy5.5) has two main fluorescence emission bands that peak at 520 and 694 nm, respectively. In the presence of $ONOO^-$, the intensity of 520 nm centered emission increased whereas that of 694 nm centered emission decreased. The fluorescence intensity ratio of the two emission bands demonstrated a strong linear relationship with $ONOO^-$ concentration.[69] These unique luminescent properties make the studied nanoprobe, a great tool to image endogenous $ONOO^-$ in cell mitochondria using ratiometric fluorescence imaging.

### 3.6 Mitochondrial micro RNA targeting imaging

Mitochondrial DNA (mtDNA) has 16.5 kb base pairs and encodes 13 complexes, and it plays an important role in regulation of immune responses.[70–72] There is only one type of mtDNA in an organism, and mtDNA possesses a unique structural characteristic, an extremely small double-stranded circular structure. However, most of the mtDNA probes are small molecules, which were proved to have low photostability and broad emission bands. And there have been very few reported imaging probes and techniques constructed by nanotechnology. Therefore, it's highly necessary to develop more ideal imaging probes, especially with the aid of mitochondrial targeting microRNA (mitomiR) that can affect mitochondrial morphology, metabolism, redox homeostasis, autophagy and apoptosis by regulating the mitochondrial gene expression. The abnormal expression of mitomiR is closely related to metabolic diseases, cardiovascular diseases, neurodegenerative diseases and tumors. Studies have found that mitomiR is involved in chemotherapy tolerance, cancer metastasis, and recurrence. Therefore, the precise *in situ* imaging of mitomiR is of great significance for exploring the physiological and pathological functions of mitomiR and disease diagnosis. Li and coworkers presented a study that makes an original contribution to mitochondrial microRNA imaging.[73] Nanoreporters based on the combination of PD (photocleavable linker into a designed DNA sensor probe) and UCNPs were synthesized using the mitochondria targeting strategy. Upconverted $NaGdF_4$:$Yb^{3+}$,$Tm^{3+}$ core–shell nanocomposites efficiently convert NIR light to ultraviolet (UV) light. During the targeting procedure, the DNA nanoreporters could be localized to mitochondria in live cells with blocked sensing function. Then, the UV light-activatable PD sensing function could be triggered noninvasively by the UV emission emitted by UCNPs upon NIR excitation at a certain time and location. To be specific, the UV emission triggers strand displacement reactions (SDRs), thus ensuring accurate mitomiR imaging at a specific location in suborganelles.

## 4. Conclusion and perspectives

Mitochondria are the main energy supply organelles in cells, the main source of intracellular reactive oxygen species, and one of the regulatory hubs of cell apoptosis. It has now been demonstrated that the dynamic changes in the mitochondrial structure and function, as well as the microenvironment in mitochondria can cause cellular energy disturbances and oxidative damage, which may result in neurodegenerative diseases, metabolic problems, cardiovascular diseases and others. Mitochondrial imaging is a useful tool to track the changes in the mitochondrial internal structure and monitor the performance of mitochondria. Used in one of the three main techniques that are used for mitochondria targeted imaging, the small molecule fluorescent probes are easy to use, water-soluble, and can be passively transported across the cell membrane and directly aggregated on active mitochondria. However, one disadvantage regarding this technique is that the performance of small molecule fluorescent probes strongly depends on mitochondrial membrane potential. The probes will fall off from mitochondria if the mitochondrial membrane potential is lost. This finding significantly limits their use and application in tracking the environmental changes in mitochondria. In contrast, nanomaterials exhibit unique properties of robust photobleaching resistance and great photostability. More importantly, they enable us to detect the changes in mitochondrial microenvironment, making them a promising solution for mitochondrial imaging.

It is also noted that more advanced microscopy techniques make a crucial impact on the development of the mitochondria imaging. The cristae of mitochondria can only be observed by simultaneously applying novel photostable mitochondrial probes and state-of-the-art microscopic imaging techniques such as Hessian SIM, STED superresolution microscopy and algorithm-assisted super-resolution imaging. Despite the fact that there has been a rapid development of mitochondria targeted imaging by using fluorescent nanoprobes, there are several limitations that need further research and study. First, nanoprobes usually require complicated sample preparation processes. Second, the broad and visible only luminescence spectra result in strong background signal and weak signal-to-noise ratio. Therefore, it is necessary to develop new probes with a narrow luminescence interval, strong photostability and good biocompatibility, which would be of far-reaching significance to the understanding of mitochondria related diseases and the development of mitochondria targeting drugs.

## Author contributions

All authors (N. Z., Q. W., S. Z., C. M., L. H., and S. L.) contributed to writing, reviewing and editing of this work and consented to the final version. All authors have read and agreed to the published version of the manuscript.

## Funding

This work was supported by the National Science Fund for Distinguished Young Scholars (No. 51825202), the National Natural Science Foundation of China (U20A20339) and the

Fundamental Research Funds for the Central Universities (AUGA5710052421).

## Conflicts of interest

The authors declare no conflict of interest.

## References

1 D. J. Pagliarini and J. Rutter, *Genes Dev.*, 2013, **27**, 2615–2627.
2 J. B. Spinelli and M. C. Haigis, *Nat. Cell Biol.*, 2018, **20**, 745–754.
3 J. Nunnari and A. Suomalainen, *Cell*, 2012, **148**, 1145–1159.
4 S. B. Vafai and V. K. Mootha, *Nature*, 2012, **491**, 374–383.
5 H. Wang, B. Fang, B. Peng, L. Wang, Y. Xue, H. Bai, S. Lu, N. H. Voelcker, L. Li, L. Fu and W. Huang, *Front. Chem.*, 2021, **9**, 683220.
6 Y. Chu, J. Park, E. Kim and S. Lee, *Materials*, 2021, **14**, 4180.
7 J. Yang, Y. Guo, M. Pistolozzi and J. Yan, *Dyes Pigm.*, 2021, **193**, 109466.
8 C. Ma, F. Xia and S. O. Kelley, *Bioconjugate Chem.*, 2020, **31**, 2650–2667.
9 H. Yuan, H. Cho, H. H. Chen, M. Panagia, D. E. Sosnovik and L. Josephson, *Chem. Commun.*, 2013, **49**, 10361–10363.
10 C. Zhang, T. Liu, Y. Su, S. Luo, Y. Zhu, X. Tan, S. Fan, L. Zhang, Y. Zhou, T. Cheng and C. Shi, *Biomaterials*, 2010, **31**, 6612–6617.
11 F. Miao, W. Zhang, Y. Sun, R. Zhang, Y. Liu, F. Guo, G. Song, M. Tian and X. Yu, *Biosens. Bioelectron.*, 2014, **55**, 423–429.
12 A. Martin, A. Byrne, C. S. Burke, R. J. Förster and T. E. Keyes, *J. Am. Chem. Soc.*, 2014, **136**, 15300–15309.
13 V. Jayashankar and S. M. Rafelski, *Curr. Opin. Cell Biol.*, 2014, **26**, 34–40.
14 T. G. Frey and C. A. Mannella, *Trends Biochem. Sci.*, 2000, **25**, 319–324.
15 C. R. Schiavon, T. Zhang, B. Zhao, A. S. Moore, P. Wales, L. R. Andrade, M. Wu, T. C. Sung, Y. Dayn, J. W. Feng, O. A. Quintero, G. S. Shadel, R. Grosse and U. Manor, *Nat. Methods*, 2020, **17**, 917–921.
16 B. Lin, Y. Liu, X. Zhang, L. Fan, Y. Shu and J. Wang, *ACS Sens.*, 2021, **6**, 4009–4018.
17 L. Zhang, J. L. Wang, X. X. Ba, S. Y. Hua, P. Jiang, F. L. Jiang and Y. Liu, *ACS Appl. Mater. Interfaces*, 2021, **13**, 7945–7954.
18 D. Ma, Q. Zong, Y. Du, F. Yu, X. Xiao, R. Sun, Y. Guo, X. Wei and Y. Yuan, *Acta Biomater.*, 2021, **135**, 628–637.
19 J. Wu, C. Han, X. Cao, Z. Lv, C. Wang, X. Huo, L. Feng, B. Zhang, X. Tian and X. Ma, *Anal. Chim. Acta*, 2022, **1199**, 339573.
20 J. Huang, D. Hong, W. Lang, J. Liu, J. Dong, C. Yuan, J. Luo, J. Ge and Q. Zhu, *Analyst*, 2019, **144**, 3703–3709.
21 A. T. Hoye, J. E. Davoren, P. Wipf, M. P. Fink and V. E. Kagan, *Acc. Chem. Res.*, 2008, **41**(1), 87–97.
22 G. Zhang, Y. Sun, X. He, W. Zhang, M. Tian, R. Feng, R. Zhang, X. Li, L. Guo, X. Yu and S. Zhang, *Anal. Chem.*, 2015, **87**(24), 12088–12095.
23 S. Jakobs, *Biochim. Biophys. Acta, Mol. Cell Res.*, 2006, **1763**(5), 561–575.
24 B. A. D. Neto, J. R. Corrêa and R. G. Silva, *RSC Adv.*, 2013, **3**(16), 5291–5301.
25 A. Rathinavelu, K. Alhazzani, S. Dhandayuthapani and T. Kanagasabai, *Tumor Biol.*, 2017, **39**, 1010428317726841.
26 M. V. Dubinin, A. A. Semenova, A. I. Ilzorkina, N. V. Penkov, D. A. Nedopekina, V. A. Sharapov, E. I. Khoroshavina, E. V. Davletshin, N. V. Belosludtseva, A. Y. Spivak and K. N. Belosludtsev, *Free Radical Biol. Med.*, 2021, **168**, 55–69.
27 P. Sancho, E. Galeano, E. Nieto, M. D. Delgado and A. I. Garcia-Perez, *Leuk. Res.*, 2007, **31**, 969–978.
28 Y. F. Song, D. Z. Liu, Y. Cheng, M. Liu, W. L. Ye, B. L. Zhang, X. Y. Liu and S. Y. Zhou, *Sci. Rep.*, 2015, **5**, 16125.
29 L. V. Johnson, M. L. Walsh and L. B. Chen, *Proc. Natl. Acad. Sci. U. S. A.*, 1980, **77**, 990–994.
30 R. L. Pan, W. Q. Hu, J. Pan, L. Huang, C. C. Luan and H. M. Shen, *Neural Regener. Res.*, 2020, **15**, 1086–1093.
31 S. A. Dyshlovoy, E. K. Kudryashova, M. Kaune, T. N. Makarieva, L. K. Shubina, T. Busenbender, V. A. Denisenko, R. S. Popov, J. Hauschild, S. N. Fedorov, C. Bokemeyer, M. Graefen, V. A. Stonik and G. von Amsberg, *Sci. Rep.*, 2020, **10**, 9764.
32 F. Auzel, *Chem. Rev.*, 2004, **104**(1), 139–174.
33 M. Haase and H. Schäfer, *Angew. Chem., Int. Ed.*, 2011, **50**(26), 5808–5829.
34 C. Liu, B. Liu, J. Zhao, Z. Di, D. Chen, Z. Gu, L. Li and Y. Zhao, *Angew. Chem., Int. Ed.*, 2020, **59**(7), 2634–2638.
35 X. Qian, Z. Gu and Y. Chen, *Mater. Horiz.*, 2017, **4**(5), 800–816.
36 Z. Sun, H. Xie, S. Tang, X.-F. Yu, Z. Guo, J. Shao, H. Zhang, H. Huang, H. Wang and P. K. Chu, *Angew. Chem., Int. Ed.*, 2015, **54**(39), 11526–11530.
37 J. Shao, H. Xie, H. Huang, Z. Li, Z. Sun, Y. Xu, Q. Xiao, X.-F. Yu, Y. Zhao, H. Zhang, H. Wang and P. K. Chu, *Nat. Commun.*, 2016, **7**(1), 12967.
38 X. Yang, D. Wang, J. Zhu, L. Xue, C. Ou, W. Wang, M. Lu, X. Song and X. Dong, *Chem. Sci.*, 2019, **10**(13), 3779–3785.
39 Q. Zhuang, H. Jia, L. Du, Y. Li, Z. Chen, S. Huang and Y. Liu, *Biosens. Bioelectron.*, 2014, **55**, 76–82.
40 F. Yu, Y. Shao and X. Chai, *et al.*, *Angew. Chem., Int. Ed.*, 2022, **61**, e202203238.
41 P. C. Saha, T. Bera, T. Chatterjee, J. Samanta, A. Sengupta, M. Bhattacharyya and S. Guha, *Bioconjugate Chem.*, 2021, **32**, 833–841.
42 Y. Cheng, F. Yang, K. Zhang, Y. Zhang, Y. Cao, C. Liu, H. Lu, H. Dong and X. Zhang, *Adv. Funct. Mater.*, 2019, **29**, 1903850.
43 X. Wu, S. Sun, Y. Wang, J. Zhu, K. Jiang, Y. Leng, Q. Shu and H. Lin, *Biosens. Bioelectron.*, 2017, **90**, 501–507.
44 O. Oladimeji, J. Akinyelu, A. Daniels and M. Singh, *Int. J. Mol. Sci.*, 2021, **22**, 5072.
45 B. Mta, L. Kai and B. Mr, *et al.*, A mitochondria-targeting lipid-small molecule hybrid nanoparticle for imaging and



 

therapy in an orthotopic glioma model, *Acta Pharm. Sin. B*, 2022, **12**(6), 2672–2682.
46 G. Gao, Y.-W. Jiang, J. Yang and F.-G. Wu, *Nanoscale*, 2017, **9**(46), 18368–18378.
47 C. Gui, E. Zhao, R. T. K. Kwok, A. C. S. Leung, J. W. Y. Lam, M. Jiang, H. Deng, Y. Cai, W. Zhang, H. Su and B. Z. Tang, *Chem. Sci.*, 2017, **8**(3), 1822–1830.
48 Q. Hu, M. Gao, G. Feng and B. Liu, *Angew. Chem., Int. Ed.*, 2014, **53**(51), 14225–14229.
49 M. H. Chen, F. X. Wang, J. J. Cao, C. P. Tan, L. N. Ji and Z. W. Mao, *ACS Appl. Mater. Interfaces*, 2017, **9**, 13304–13314.
50 A. M. Aleardi, G. Benard, O. Augereau, M. Malgat, J. C. Talbot, J. P. Mazat, T. Letellier, J. Dachary-Prigent, G. C. Solaini and R. Rossignol, *J. Bioenerg. Biomembr.*, 2005, **37**, 207–225.
51 D. V. Kolygina, M. Siek, M. Borkowska, G. Ahumada, P. Barski, D. Witt, A. Y. Jee, H. Miao, J. C. Ahumada, S. Granick, K. Kandere-Grzybowska and B. A. Grzybowski, *ACS Nano*, 2021, **15**, 11470–11490.
52 X. Li, X. Guo, L. Cao, Z. Xun, S. Wang, S. Li, Y. Li and G. Yang, *Angew. Chem., Int. Ed.*, 2014, **53**, 7809–7813.
53 J. L. Tang, C. Y. Li, Y. F. Li and C. X. Zou, *Chem. Commun.*, 2014, **50**, 15411–15414.
54 K. Y. Tan, C. Y. Li, Y. F. Li, J. Fei, B. Yang, Y. J. Fu and F. Li, *Anal. Chem.*, 2017, **89**, 1749–1756.
55 B. Chu, A. Wang, L. Cheng, R. Chen, H. Shi, B. Song, F. Dong, H. Wang and Y. He, *J. Nanobiotechnol.*, 2021, **19**, 187.
56 J. Deng, K. Wang, M. Wang, P. Yu and L. Mao, *J. Am. Chem. Soc.*, 2017, **139**, 5877–5882.
57 J. H. Liu, R. S. Li, B. Yuan, J. Wang, Y. F. Li and C. Z. Huang, *Nanoscale*, 2018, **10**, 17402–17408.
58 F. Du, Y. Min, F. Zeng, C. Yu and S. Wu, *Small*, 2014, **10**, 964–972.
59 J. Qiao, Z. Liu, Y. Tian, M. Wu and Z. Niu, *Chem. Commun.*, 2015, **51**, 3641–3644.
60 C. Szabo, *Nat. Rev. Drug Discovery*, 2007, **6**, 917–935.
61 D. J. Lefer, *Proc. Natl. Acad. Sci. U. S. A.*, 2007, **104**, 17907–17908.
62 W. Guo, J. T. Kan, Z. Y. Cheng, J. F. Chen, Y. Q. Shen, J. Xu, D. Wu and Y. Z. Zhu, *Oxid. Med. Cell. Longevity*, 2012, **2012**, 878052.
63 S. K. Bae, C. H. Heo, D. J. Choi, D. Sen, E.-H. Joe, B. R. Cho and H. M. Kim, *J. Am. Chem. Soc.*, 2013, **135**, 9915–9923.
64 X. Wang, J. Sun, W. Zhang, X. Ma, J. Lv and B. Tang, *Chem. Sci.*, 2013, **4**, 2551–2556.
65 Y. Chen, C. Zhu, Z. Yang, J. Chen, Y. He, Y. Jiao, W. He, L. Qiu, J. Cen and Z. Guo, *Angew. Chem., Int. Ed.*, 2013, **52**, 1688–1691.
66 S. Wen, J. Zhou, K. Zheng, A. Bednarkiewicz, X. Liu and D. Jin, *Nat. Commun.*, 2018, **9**, 2415.
67 X. Li, H. Zhao, Y. Ji, C. Yin, J. Li, Z. Yang, Y. Tang, Q. Zhang, Q. Fan and W. Huang, *ACS Appl. Mater. Interfaces*, 2018, **10**, 39544–39556.
68 S. Xu, G. Zheng and K. Zhou, *Anal. Biochem.*, 2022, **640**, 114545.
69 K. Yang, L. Hou, Z. Li, T. Lin, J. Tian and S. Zhao, *Talanta*, 2021, **231**, 122421.
70 K. Ishikawa, K. Takenaga, M. Akimoto, N. Koshikawa, A. Yamaguchi, H. Imanishi, K. Nakada, Y. Honma and J. Hayashi, *Science*, 2008, **320**, 661–664.
71 K. McArthur, L. W. Whitehead, J. M. Heddleston, L. Li, B. S. Padman, V. Oorschot, N. D. Geoghegan, S. Chappaz, S. Davidson, H. San Chin, R. M. Lane, M. Dramicanin, T. L. Saunders, C. Sugiana, R. Lessene, L. D. Osellame, T. L. Chew, G. Dewson, M. Lazarou, G. Ramm, G. Lessene, M. T. Ryan, K. L. Rogers, M. F. van Delft and B. T. Kile, *Science*, 2018, **359**, 883–895.
72 K. Gao, M. Cheng, X. Zuo, J. Lin, K. Hoogewijs, M. P. Murphy, X. D. Fu and X. Zhang, *Cell Res.*, 2021, **31**, 219–228.
73 J. Zhao, Z. Li, Y. Shao, W. Hu and L. Li, *Angew. Chem., Int. Ed.*, 2021, **60**, 17937–17941.